Acta of Bioengineering and Biomechanics
Vol. 13, No. 3, 2011

Original paper

Procedure of generating the individually matched bone scaffolds

JAKUB SŁOWIŃSKI*

Institute of Materials Science and Applied Mechanics, Wrocław University of Technology, Poland.

The pace of modern life forced continuous high readiness and proper condition of motion systems on human beings. The techniques used in medicine and orthopaedics enable treatment of even highly complicated injuries and pathological states. One of them involves the use of bone scaffolding – the technique being intensively developed, which seems to have a promising future. Based on a numerical modelling, it is possible to match that type of implant to the needs of individual patient, with consideration for both biomechanical factors (patient weight, bone size and its defects) and the applicable implantation techniques. Vast possibilities are offered by the application of the finite element method as a technique enabling verification of an implant with the individually matched geometry and material. The paper presents the procedure aimed at generating the bone scaffold structure that enables the stresses created in the contact places of implant with the surrounding bone tissue to be reduced. High stresses may lead to local damages to the tissue and, in extreme cases, to the destruction of a scaffold. The present procedure is based on the theory of genetic algorithms and, due to several models widely known in biomechanics, allows stresses in places of bone contact with implant to be significantly reduced.

Key words: *tissue scaffolds, tibia bone, finite element method*

1. Introduction

A human motion system, both active and passive, is highly complicated in terms of biology and mechanics. The fast pace of life in highly developed countries and frequently insufficient health care in the developing countries may lead to malfunctions of that system. In Poland alone, in 2007, almost 20 thousand bone fractures resulting from injuries were recorded [1]. The factors causing damage to bone system involve, among others, neoplastic diseases and genetic disorders such as the intrinsic bone brittleness (*osteogenesis imperfecta*) [2].

In the United States, over 450 thousand of bone transplantations are performed yearly (2.2 M all over the world). Their aim is to supplement bone decrements both after injury and after removal of pathological tissues, mainly the cancerous ones [3].

The process of damaged bone tissue repair consists in restoring continuity and/or filling in the decrements. Fillings are presently accomplished by bone tissue transplants from a tissue bank (allotransplantation) or collected directly from the patient's own body (autotransplantation), e.g., from an iliac ala bone [4]. The autotransplantation procedure, despite the development in operation techniques, poses high risk of blood loss, extended time of operation and possible infection. Essential limitation of that technique is the possibility of collecting only a small bone fragment, which not always is adequate for a patient [5]. That problem can be solved allogenic transplantations, i.e., by using a material from foreign donor (human). However, an essential disadvantage of such a procedure is the risk of rejecting the transplant and the possibility of transferring the donor's disease to a recipient. This type of treatment is also characterised by a slower recovery than in the case of autograft and the

* Corresponding author: Jakub Słowiński, Institute of Materials Science and Applied Mechanics, Wrocław University of Technology, ul. Smoluchowskiego 25, 50-370 Wrocław, Poland. Tel: +48 71 3202899, fax: +48 71 3211235, e-mail: jakub.slowinski@pwr.wroc.pl

Received: May 23rd, 2011
Accepted for publication: July 29th, 2011

necessity of applying the immunosuppressive medicines [6], [7]. Transplantations of animal tissues (xenograft) are considered as well; however, this method also poses some risk [8].

At present, the application of bone autografts constitutes the golden standard in treating and rebuilding the bone tissue structure [9], [10]. However, it has to be stressed that the bone material is not always available and the patient's health frequently does not allow any additional surgical interventions. The application of scaffolds significantly raises the treatment possibilities because of their ready availability, minimizes the risk of after-surgery complications and excludes the use of immunosuppressive medicines. The bone scaffolds have essential advantage of being specially prepared, which facilitates both performing the operation and enables better patient's recovery.

For the first time the bone scaffolds were given to patients as medication at the end of the 1980s, the beginning of the 1990s of the twentieth century. Bone decrements in animals under laboratory conditions were successfully treated using the ceramic materials sown with mother cells of bone marrow [11]. These cells have the pluripotent capabilities, hence they can be the incipience of every type of organism tissue, from which they are isolated. Some researchers reveal that it is possible to use epithelium cells, due to their active participation in angiogenesis processes, for rebuilding bone tissue [12].

2. The aim of the study

The main aim of this study was to establish, based on the theory of genetic algorithms, the procedure for finding some optimal structures of bone scaffold. These optimised implants should be more useful in repairing skeletal tissues because they mimic natural bone much more accurately than non-optimised structures.

3. Material and method

In order to achieve individual purposes, numerical models of relevant structures were prepared. As the first one the numerical model of tibia (shinbone) was created and constructed. Data necessary for the reproduction of anatomically correct bone geometry were collected by digital scanning the surface of the tibia physical model prepared by Sawbones® firm in the Department of Biomedical Engineering and Experimental Mechanics at the Mechanical Engineering Faculty of the Wrocław University of Technology. The model was created as a result of averaging the data coming from human bone anthropological measurements both in regard to geometrical parameters and their mechanical properties. The surface map was then transferred into the Ansys v.11 program, creating a basis for a full three-dimensional model of human tibia (figure 1).

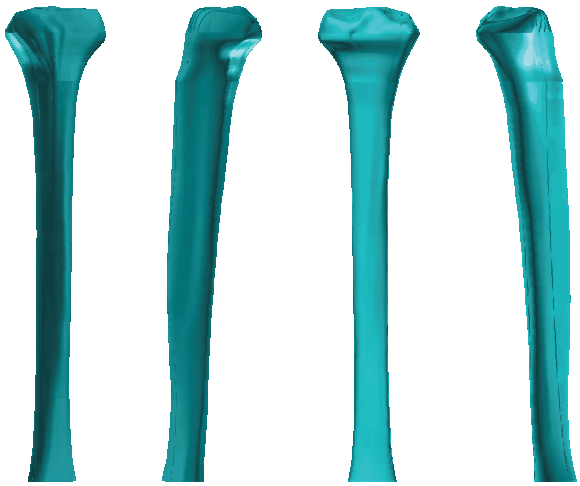

Fig. 1

In the next step, the geometrical model was divided into a net of finite elements. During digitizing process the higher-order element of the *hexa-hedra* type with 20 nodes and 3 degrees of freedom in each node, i.e. translation in the x, y and z directions, was utilised. The use of such elements enabled creation of a network from smaller number of elements while keeping up to the good representation of the complex model shape. The model consisted of 23,224 elements, which could be translated into 101,657 nodes. In order to increase the accuracy of further calculations, the division into a dense bone tissue and a spongy bone tissue, compatible with the real division, was introduced into the model developed. The division is based on the analysis of the X-ray images of the modelled skeleton fragment. Additionally, the division network created in an automatic process was manually modified in the areas where the stress concentrations were expected. For the modelled materials the isotropic material characteristics were assumed, but the type of the finite element used in the digitizing process enables a future definition of a material with anisotropic characteristic. Nevertheless, such a step would require additional tests showing directional characteristics of the bone tissue tested. External layer of the model was defined as a dense bone tissue, the mechanical properties of which were selected according to the

available bibliography data: Young modulus equal to 18,600 MPa, and Poisson's ratio to 0.3. Correspondingly, the bone interior, understood as a supplementation of the model, was described by the material properties typical of a spongy bone tissue, i.e., $E = 482$ MPa, and $\nu = 0.42$ [13].

During the procedure, the discrete model was fastened and next loaded with external forces. The fixing of the model was accomplished by eliminating all degrees of freedom of the further end of the tibia nodes (figure 2).

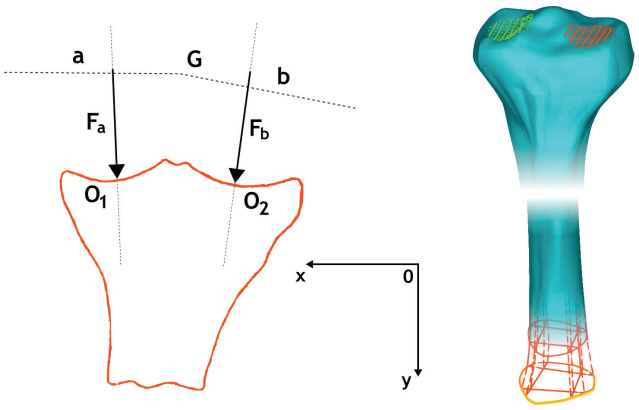

Fig. 2

The loading of the tibia was accomplished by applying a set of forces at the condylar surfaces of the tibia: medial F_a and lateral F_b (figure 2). Based on the loading model of a knee joint known from literature and on the analysis of the load state of tibia in the supporting phase of walk [14], [15], 14 cases of external forces acting in the frontal plane and expressing individual stages of the supporting walk phase were examined (table 1). It was decided to disregard in the tests the forces generated by the interactions between iliotibial band and the peroneal part of the lower limb. Such an approach was possible, considering the character of the work conducted. The aim of the research was to develop the method enabling searching for the structures of a bone implant, and not to exactly reproduce the loading state of the knee joint and the resultant distribution of stresses, strains and displacements in the tibia epiphysis and in the bone implant. Pathological state of varus loading (table 2) was examined according to the rule presented by ŚCIGAŁA [16]. Thus, the varus deformity of tibia was achieved by the asymmetric rescaling of forces loading the condylar surfaces without mapping the changes in the model geometry. Such a solution enables the mapping of a tibia position change in the case of varus deformity – its outward deflection in relation to mechanical axis of the lower limb. The above situation leads to a change in contact surface within the condyles of knee joint, hence to its increase on the medial side and a decrease on the lateral side.

Table 1. Values of forces used for loading tibia during simulation (normal tibia)

Load case	Lateral condyle; F_A		Medial condyle; F_B	
	FX	*FY*	*FX*	*FY*
1	9	186	19	558
2	25	538	17	497
3	24	518	23	662
4	20	435	25	725
5	15	331	43	1242
6	–	–	50	1449
7	–	–	53	1532
8	–	–	35	1014
9	–	–	31	890
10	–	–	37	1077
11	10	228	50	1449
12	28	621	55	1594
13	33	725	44	1284
14	23	497	16	455

Table 2. Values of forces used for loading tibia during simulation (tibia vara)

Load case	Lateral condyle; F_A		Medial condyle; F_B	
	FX	*FY*	*FX*	*FY*
1	3	47	67	1562
2	7	135	60	1392
3	7	130	81	1854
4	6	109	88	2030
5	4	83	152	3478
6	–	–	177	4057
7	–	–	187	4290
8	–	–	124	2839
9	–	–	109	2492
10	–	–	131	3016
11	3	57	177	4057
12	8	155	194	4463
13	9	181	155	3595
14	7	124	56	1274

Using the full model of tibia, calculations were made, thereby effecting a distribution of nodal displacements for each case of loading, i.e., for each stage of the supportive walk phase. Next, the geometry of a full model of tibia was modified. As a result of this operation the volume of the proximal epiphysis and metaphysis and their original geometry were retained. The partition of the retained part also remained unchanged, and the numbering of nodes and elements in particular. The model in a new shape comprised 5,616 elements, which were translated into 5,162 nodes. A medical character of the procedure was responsible for such an action (patient's welfare), it was necessary

to accomplish subsequent tasks in the shortest possible time.

The numerical model of tibia obtained was used in the simulation procedure based on an algorithm of adaptive rebuilding of bone tissue known from literature [17]. The aim of that stage of the simulation based on the algorithm mentioned was to determine the density changes and Young modulus in bone tissue in the area of the proximal epiphysis of tibia under the external loads applied. All parts of the numerical model, according to resolutions of the Carter procedure, were provided with the same material properties, i.e., $E = 482$ MPa and $\nu = 0.3$ [17]. Also the density of bone tissue with the initial value of 0.5 g/cm^3 was given. The model modified as above was next loaded. The process was conducted using previously calculated nodal displacement for the full bone model. Their values were described for all nodes in a way enabling their reading in the modified model, while keeping the same numbering of nodes. That way in the part of the model subjected to geometry modification, all 14 phases of tibia loading were reproduced using the displacements.

In the first stage of the procedure for each i case of loading, the main stresses σ_i and main deformations ε_i were calculated, and in the next step, the energy of strain U_0 was determined.

$$U_0 = \frac{1}{2}\Sigma_i \sigma_i \varepsilon_i \,. \tag{1}$$

With the known density of bone tissue, in each point of the model, the deformation energy density U and the effective stress were determined:

$$U_0 = \frac{U_0}{\rho}, \tag{2}$$

$$\sigma_{\text{ef}} = \sqrt{2E_i U_i} \tag{3}$$

where:

E_i – Young's modulus for subsequent iterations of calculations,

U_i – the energy density of strain for subsequent phases of loading.

In the next step, the value of mechanical stimulus for each point of the model was determined:

$$\Psi = (\Sigma_i^N n_i \sigma_i^m)^{\frac{1}{m}}, \tag{4}$$

where:

N – the number of all loading cases,

n – the number of cycles of loading case i,

m – the coefficient determined experimentally.

The character and rate of adaptation changes $\dot{r}_m$ in bone tissue depend on the value causing remodelling of the mechanical stimulus:

$$\dot{r}_m = \begin{cases} c \cdot (\Psi - \Psi_{\text{avg}}) + c \cdot w & (\Psi - \Psi_{\text{avg}} < -w) \\ 0 & (-w \le \Psi - \Psi_r \le +w) \\ c \cdot (\Psi - \Psi_{\text{avg}}) - c \cdot w & (\Psi - \Psi_{\text{avg}} > +w) \end{cases} \tag{5}$$

where:

c – the slope coefficient of the curve representing the rate of bone tissue adaptation changes,

w – the half-width of the sluggish zone,

Ψ – the value of the mechanical stimulus,

Ψ_{avg} – the average value of the mechanical stimulus.

Under the influence of mechanical stimulus of too low value on the bone tissue, the processes of resorption predominate, leading to a drop in tissue density and its gradual atrophy. In the situation, where stimulus exceeds a certain defined value, the processes of new tissue formation begin to predominate, resulting in an increase in its density and its mechanical parameters. A central range of the stimulus values is referred to as the so-called lazy zone. Within its borders the adaptive changes of bone tissue are in the dynamic equilibrium, which is translated into preserving the density value, and thus the Young modulus value in a given point of the model. The lazy zone spreads symmetrically around an average value of the mechanical stimulus in the area of 50% of its value ($W = 0.25\ \Psi_{\text{avg}}$). Based on the experimental data the average stimulus for human tibia was determined within the range of 30–70 MPa, while the coefficient m amounted to 4. Determination of the rebuilding rate coefficient $\dot{r}_m$ allowed reaching a subsequent stage, where the active surface of bone tissue (BS/TV) was calculated. According to this concept, we deal with that part of bone surface in which the adaptation processes take place. The parameter BS/TV was determined on the basis of the relationship proposed by MARTIN [18]. It was approximated by polynomials in the procedure developed. A subsequent part of the procedure consisted in determining the value of density for a bone adapting to the loading conditions (6). The density was defined as the quotient of the BS/TV coefficient of the previous density in a given point of model and the coefficient $\dot{r}_m$. The coefficient k determining the part of the active surface participating in the functional adaptation was equal to unity.

$$\dot{\rho} = k(BS/TV)\rho_t \dot{r} \,. \tag{6}$$

Then use was made of the relationship proposed by Carter and Beaupré and connecting the Young modulus value of bone tissue with its density:

$$E = \alpha\rho^{\beta} . \tag{7}$$

In accordance with the experiments performed by Carter and Beaupré, the value of the multiplier α of the exponent β is being changed depending on the density of bone tissue. Their values are as follows: $\alpha = 2704$ and $\beta = 2.5$ at $\rho \leq 1.2$ g/cm^3 and $\alpha = 2385.1$ and $\beta = 3.2$ at $\rho > 1.2$ g/cm^3. The new values of individual parameters calculated as a result of the present simulation steps were next assigned to all elements of the model. Finally, we obtained the model of tibial bone epiphysis with probable distribution of material properties achieved as a response to the specified load conditions.

4. Model of a spongy bone tissue section

In order to develop a model of bone tissue section, an interactive procedure was prepared, which allowed determination of the basic features of scaffold as well as its precise localisation in a bone volume. The parameters of scaffold involve:

- geometrical dimensions – side length (assuming that scaffold is an ideal substitute for cubical bone fragment),
- the diameters of small beams triggering the development of a scaffold – their minimum value assumed was 0.6 mm,
- the number of small beams in a model – their minimum value assumed was 3 beams per side, i.e., 54 beams creating a model,
- the length of a single small beam in an initial model – its minimum value assumed was 2.4 mm.

After defining the basic parameters of scaffold, it was necessary to indicate a bone wall, through which an access to the removed part of a bone tissue for the benefit of the scaffold was to be made. The position of an implant was defined both in the frontal cutting plane and in the transverse section plane. The positioning of scaffold in the front cutting plane was accomplished by selecting one of the points oriented outwards the model, along the axis parallel to the long bone axis. One point defined localisation of lower cubical surface of the scaffold volume, perpendicular to the long axis of the bone and to the frontal cutting plane. The positioning of an implant in the transverse section plane was made in two stages. In the first one, the cross-section of tibial bone epiphysis was generated at the height previously indicated by selecting the position of lower scaffold surface. Then, at the defined intersection lying in the screen plane, the implant was positioned along two axes perpendicular to the long bone axis (figure 3). Interactive part of the program was finished after approving the correctness of actions made by a user. The next step in the procedure presented was taken to create a bone tissue section model together with its closest surroundings. The dimensions of the section were equal to those of the fragment of bone tissue removed from epiphysis in favour of the scaffold. The model of bone section was built of two volumes – the surroundings and the proper bone section located centrally inside it. A greater part of the volume was hollowed out, so a smaller one was the complement to it. The volume of bone section was next reduced symmetrically, so it was 0.01 of the initial section side length on each side away from the surroundings. In the way described, the section was hanged inside the surrounding volume (figure 4) and the mutual junction of both volume walls was modelled by defining the contact between adjacent nodes of the section and its surroundings. The division into finite elements was made with the use of a cubical part of 8 nodes and three degrees of freedom in each node, i.e., translation into the directions x, y and z. Modelling the section along with its surroundings was related to the need of its loading and then the scaffold was inserted in its place by means of displacements

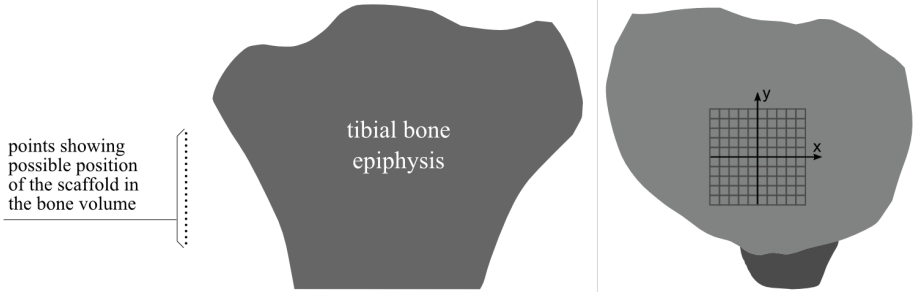

Fig. 3

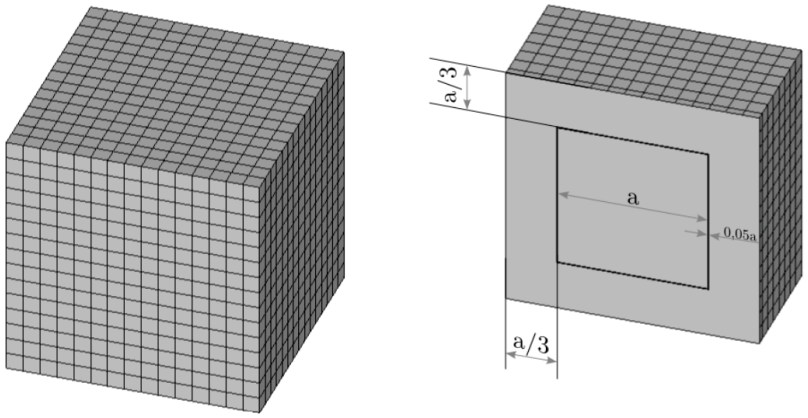

Fig. 4

(previously obtained in the full model). Imposing the loads in the form of displacements directly to the section (without the surroundings) would exclude the possibility of reading the displacement values in the indicated points of the model, created as a result of this loading. The application of the above solution, with the additional surroundings, allowed the problem to be overcome and was compatible with real conditions of loading the structures of this type in an organism. The use of the above numerical model of a bone tissue section could be explained by the possibility of observing the results in the area of the bone scaffold implantation and by the need for minimising the time necessary for performing calculations.

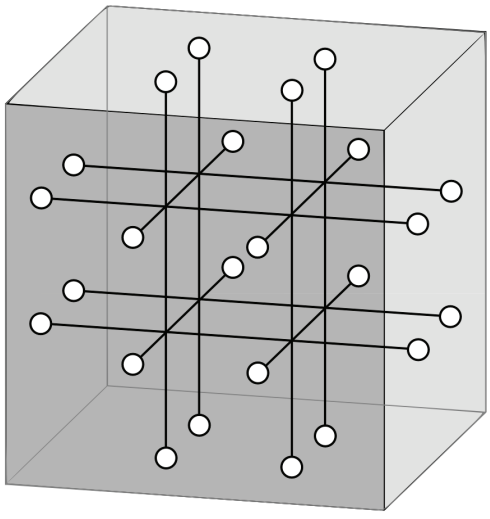

Fig. 5

The co-ordinate tables for all points creating the model were prepared and next used for making the so-called path in a model of tibia epiphysis. The path is a collection of points subsequently defined in the model (of a definite localisation), where the previously calculated specific properties such as material density or stress values are read. That way, from the section model the following quantities were collected and filled in the table: node displacement values in all three directions, as well as material densities and Young's modulus. Subsequently, the nodal displacements collected from the model of proximal epiphysis were attached to nodes belonging to the elements of the surroundings of the proper section, and the phenomenon of the contact between the neighbouring nodal pairs of section–surroundings was modelled. That way it was possible to determine the nodal reactions in selected points of the model (figure 5), which were next compared with data collected from simulation performed with the use of the bone scaffold model.

5. Bone scaffold model

The present procedure has been developed for metallic scaffold of the beam type. The application of metallic materials, among which titanium or its alloys is most suitable, seems to be justified because of their high fatigue strength as well as well-known features of titanium as biomaterial. The bone scaffold model has been developed as a result of the matching procedure activity, which was based on a specially written genetics. The initial structure was a model with a construction similar to one of the contemporary scaffold types. It was generated in the form of a three-dimensional regular set of bars oriented perpendicularly to one another. A basic fault of that structural solution is the implant isotropy. The regular and repeatable structure is clearly visible against the background of asymmetric, complex state of stresses in the bone tissue section to be replaced with scaffold. In terms of mechanical properties, the model was given

the features of titanium, the metal known as a biomaterial of outstanding features, for years used for the production of bone implants. The division into finite elements was performed using beam elements, i.e., binodal elements with 6 degrees of freedom in a node (translation and rotation for the x, y and z directions).

For the sake of easy orientation in the description of the results obtained, a division into the scaffold model walls is introduced. The term "wall" refers to the mental surface created by the external scaffold points – in practice it is a surface to which the contact points of bone tissue and the implant belong (figure 6).

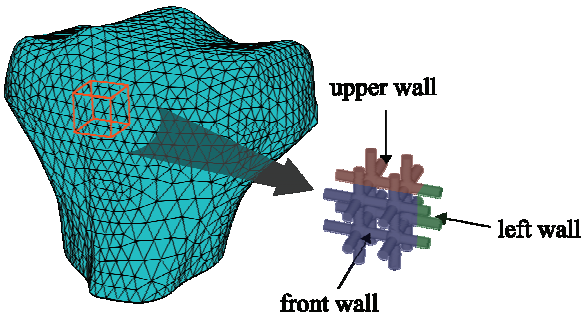

Fig. 6

6. Matching procedure function

The matching process of scaffold structure was conducted with the use of a program built based on the procedures typical of genetic algorithms. This approach to such complex issues as the matching of structure enabled seeking for solutions in the large space, while keeping up the moderate time of calculations.

The criterion of matching the structure to conditions of co-operation with bone tissue adapted in the program run was the value of nodal reaction forces calculated in defined points of the scaffold structure. The remaining structural data, such as the material, geometrical dimensions and general characteristic of the structure, were assumed a priori. Comparison of reaction values produced in the generated structure with those obtained for the bone tissue model enabled determining the value of the accommodation function, hence determining the degree of the structure change.

The basic scaffold model constituted the first initial link in the matching procedure. Its aim was to create a bone scaffold being individually matched to a patient's needs, expressing themselves in the structure of spongy bone being created as a result of loading the bone in the area of the proximal epiphysis of tibia. Making use of the possibilities offered by the environment of the Ansys program enabling creation of macros and procedures, my own program based on genetic algorithm theory was developed. The idea of genetic algorithms and calculations based on the assumptions of the Carl Darwin's theory of evolution originated in the second half of the 20th century. In the 60ties, the concept of evolution strategies in calculations was introduced by Ingo Rechenberg and was subsequently developed by several research teams. In 1975, John Holland in his work *Adaptation in natural and artificial systems* introduced the concept of genetic algorithm (GA) and wrote the first such an algorithm. The issue developed for years has led to the creation of many helpful tools utilised both for seeking for solutions and for widely understood optimisation. In the procedure of seeking for better matched scaffold structure, the binary coding was applied, the selection of which depended on the type of implant model building organisation. That classical type of coding defines the model building very well and allows its simple modifications. The reproduction of each model structure consisted in generating the basic model and subsequent modifying the position of internal points (figure 7). For that purpose, a genotype of a singular model was generated in the form of zero-one code (figure 8). The position of each of the internal implant model points was coded in 12 subsequent fields of genotype series. The 12 fields were uniformly divided into 3 sections corresponding subsequently to the position x, y, z in the Cartesian coordinate system. In each section, the first field defined a sign of point displacement in relation to the initial position. Three further fields (called the displacement bits) defined the distance of shifting–coding of that

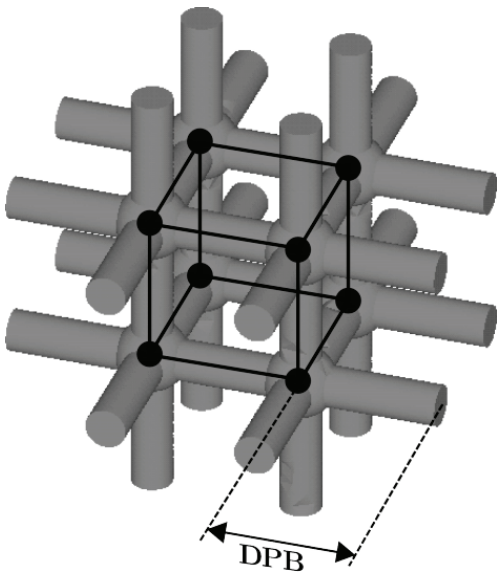

Fig. 7

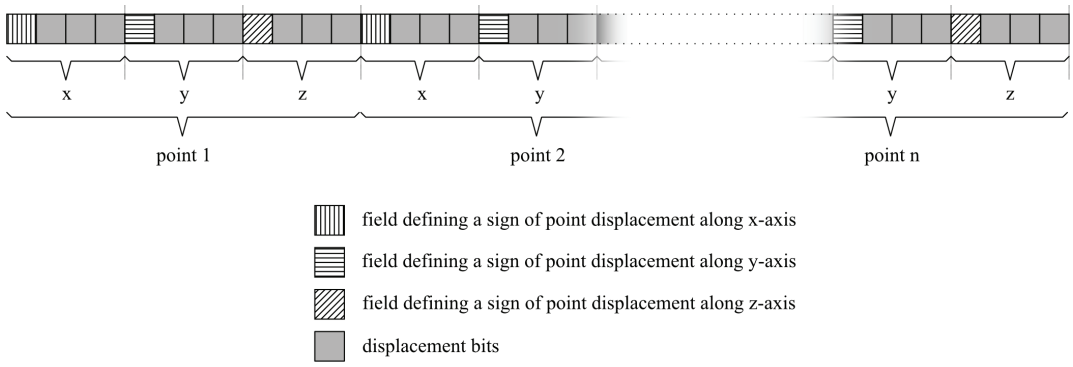

Fig. 8

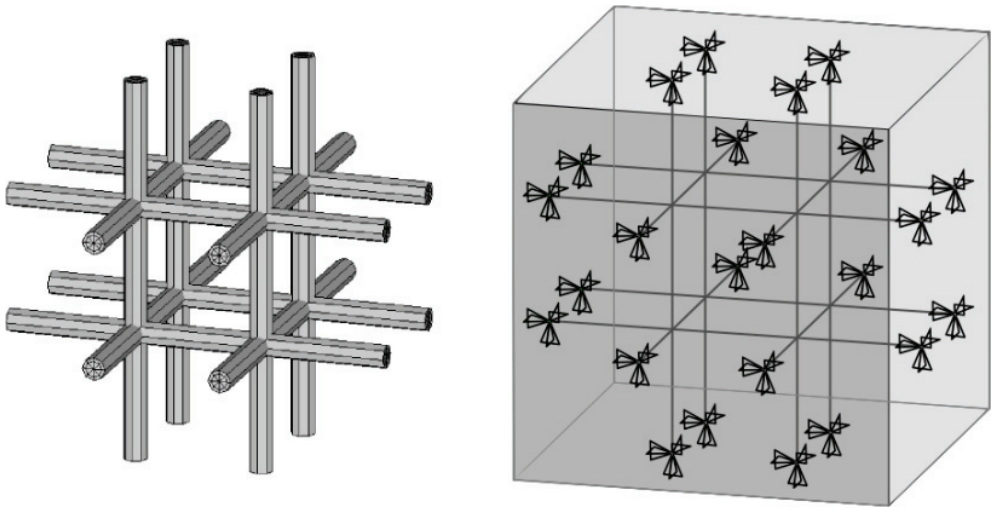

Fig. 9

value by summing up the values of those fields and multiplying it by a constant segment of the distance. Length (D) of that segment was defined as:

$$D = \frac{0.25 \cdot DPB}{LBP}, \tag{8}$$

where:

DPB – the length of a singular beam (figure 7),

LBP – the number of the shift bits.

As a result, the maximum possible shift of a node in the solution proposed amounted to 0.25 of the singular beam of the basic scaffold, and its minimum value was equal to the maximum value divided by LBP, the value being experimentally fixed as the level of 3. Such an approach excluded both the possibility of crossing the scaffold beams and the superposition of its internal points. The number of genes in genotype (DG) depended on the number of internal points (LP), which could change their positions in the process of seeking for the best matched structure, and on the number of shift bits (LBP), i.e., the number of bits coding the shift:

$$DG = 3 \cdot LP \cdot (LBP + 1). \tag{9}$$

In the model proposed, the length of genotype amounted to 96 bits for each model taking part in calculations. The matching procedure acting upon the scaffold model was divided into blocks, within which the defined steps of the genetic algorithm were executed. In the first block, the original population was generated through multiplications of the initial scaffold structure and the introduction of random changes within the position of internal points of an implant. Each of the individuals constituted a structural variation of the scaffold, for which the simulations of reaction forces' distribution in the external nodes were performed. The model loading was accomplished by applying the displacements read from the model of tibia epiphysis only on the external nodes of scaffold (figure 9). Model definition in the above described way produced a good representation of the real situation of carrying loads by the scaffold placed inside a bone. The scaffold implanted in a bone interior is being strained under the influence of moving walls of its surroundings, which in turn is displacing as a result of external loads' action.

Each of the models developed was then loaded with displacements in external nodes (the position which was not changing during the procedure). These were the displacements of the same values applied to the points with identical coordinates as in the case of the section model. That stage of the procedure ended with calculating the reaction forces' distribution in the loaded nodes. In order to define the degree of change in the newly created structures, i.e., the phenotype changes, the so-called adaptation function *SF* was introduced, being actually the phenotype value of each individual. Its general form is represented by formula (10). The value of phenotype for each individual was calculated in several steps:

1. The value of reaction forces generated in external points of scaffold at each of its walls in all loading phases was calculated; within each wall the forces were totalled.
2. Differences between the total values of reaction forces obtained in the scaffold model and the values of reaction forces obtained from the section model for the corresponding points were calculated.
3. The modules of the differences were calculated – 6 components were achieved (one for each wall).
4. The values calculated were totalled: (11)–(16).

In each of the present equations, *n* defines the number of nodes, where reaction force values were read (within one wall). In an ideal case, the value of phenotype should be equal to zero, indicating that no stress concentrations appear at the bone tissue–implant interface. In such a case, the scaffold would ideally imitate bone tissue, providing for continuity in the stress pattern:

$$SF = f^f + f^t + f^l + f^p + f^d + f^g, \qquad (10)$$

where:

f^f – difference in reaction forces between scaffold and bone section for the front wall,

f^t – difference in reaction forces between scaffold and bone section for the rear wall,

f^l – difference in reaction forces between scaffold and bone section for the left wall,

f^p – difference in reaction forces between scaffold and bone section for the right wall,

f^g – difference in reaction forces between scaffold and bone section for the upper wall,

f^d – difference in reaction forces between scaffold and bone section for the lower wall.

$$f^f = \Sigma_{i=1}^{n} | f_i^{fs} - f_i^{fw} |, \qquad (11)$$

where:

f_i^{fs} – the number of nodes in the front wall of scaffold, where reaction force value is read,

f_i^{fw} – the number of nodes in the front wall of section, where reaction force value is read.

$$f^t = \Sigma_{i=1}^{n} | f_i^{ts} - f_i^{tw} |, \qquad (12)$$

where:

f_i^{ts} – the number of nodes in the rear wall of scaffold, where reaction force value is read,

f_i^{tw} – the number of nodes in the rear wall of section, where reaction force value is read.

$$f^l = \Sigma_{i=1}^{n} | f_i^{ls} - f_i^{lw} |, \qquad (13)$$

where:

f_i^{ls} – the number of nodes in the left wall of scaffold, where reaction force value is read,

f_i^{lw} – the number of nodes in the left wall of section, where reaction force value is read.

$$f^p = \Sigma_{i=1}^{n} | f_i^{ps} - f_i^{pw} |, \qquad (14)$$

where:

f_i^{ps} – the number of nodes in the right wall of scaffold, where reaction force value is read,

f_i^{pw} – the number of nodes in the right wall of section, where reaction force value is read.

$$f^g = \Sigma_{i=1}^{n} | f_i^{gs} - f_i^{gw} |, \qquad (15)$$

where:

f_i^{gs} – the number of nodes in the upper wall of scaffold, where reaction force value is read,

f_i^{gw} – the number of nodes in the upper wall of section, where reaction force value is read.

$$f^d = \Sigma_{i=1}^{n} | f_i^{ds} - f_i^{dw} |, \qquad (16)$$

where:

f_i^{ds} – the number of nodes in the lower wall of scaffold, where reaction force value is read,

f_i^{dw} – the number of nodes in the lower wall of section, where reaction force value is read.

Thanks to fixing the value of the adaptation function *SF* for each individual of the original generation, it was possible to sort out individuals according to the phenotype value. The known bubble sort algorithm was applied here. Thereafter, the subsequent step of procedure, i.e., selection, took place. The selection is one of the most important stages of the genetic algorithm, as it allows selection of those individuals from a population, which are best suited to the solution sought for. In the present procedure, the selection was accomplished by the roulette wheel method [19]. It consists in assigning

each individual a section of roulette wheel of the size proportional to the value of the adaptation function of a given individual. Individual pairs were sampled by means of the generated roulette wheel in the quantity equal to the number of individuals in population. The sampled parent individuals allowed a descendant population to be created, which was achieved as a result of the individual crossing operation. That stage consisted in random cutting of a genotype chain in both individuals of a given pair (in the same place) and changing the fragments in such a way as to obtain two descendant individuals inheriting features from both parents (figure 10). Finally, only one individual sampled from the created pair was passing to the descendant population (figure 11). Additionally, in order to increase the population variety and at least partly prevent reaching the convergence too fast, the genotype mutation was introduced with the probability of appearance equal to about 1%. In the case of the binary coding applied, the right type of mutation was the *bit-flip* procedure [19], consisting in inversion of the random genotype fragment in randomly selected descendant individual. The new descendant population achieved as a result of the genetic recombination was overwriting individuals from the parent population and the procedure initiated subsequent iterations.

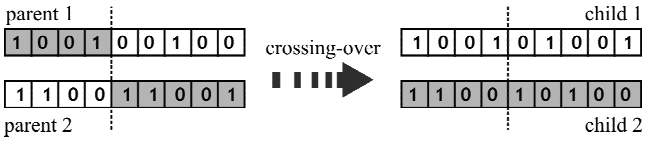

Fig. 10

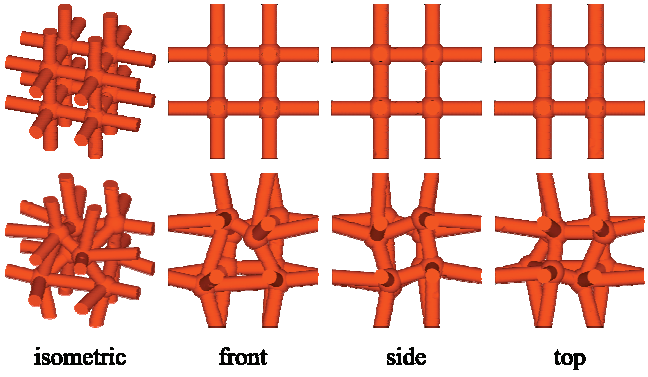

Fig. 11

7. Discussion

It has been confirmed that optimised structures are different from basic ones. The procedure developed allows us to find the implant structure best adapted to individual patient in a relatively short time (several hours). These structures mimic trabecular bone much better than regular basic structures. During simulation the characteristic distribution of trabeculae was observed. There was a tendency to create a triangle wave, mostly in the direction parallel to the long axis of bone (figure 12).

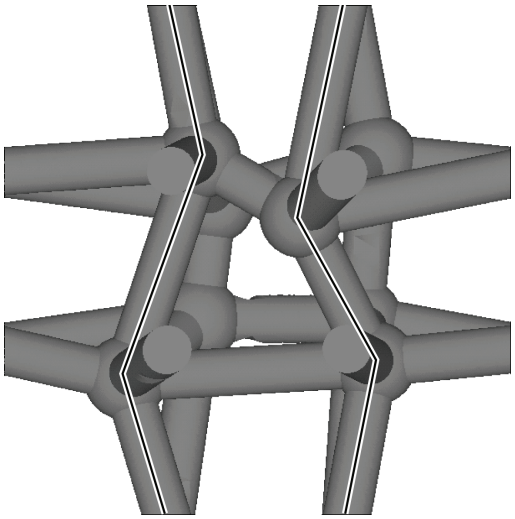

Fig. 12

The value of the adaptation function was changed mostly in the early generations of the algorithm. This means that even minimal deviation from the basic structure increases its matching to the trabecular bone. Therefore the use of symmetric trabecular scaffold structure should be avoided in contrast to [20], where only regular structures were presented.

In the present bone scaffold, the coordinates of all internal free points were described using displacement bits. This method is unique and allows us to achieve a final solution in relatively short time. The whole code was specially written in APDL language in contrast to [21], where MATLABoptimization toolbox was used.

During the work it was assumed that the population of an optimum size is constituted by 30 individuals, i.e., 30 models of scaffold structure. A smaller size, on the level of 20 individuals, did not allow us to achieve satisfactory results, mainly because of too low variety of individuals. An increase in the number of population individuals over the defined limit (up to 40 individuals) caused a significant extension of the calculation time and led to only minor improvement of the results. Due to the algorithm constructed it was possible to obtain the structures, in the number equal to the number of iterations in the program, that could be a functional substitute for a bone tissue section. In

each generation, a leading structure in terms of adaptation degree was selected and its genotype was written in the external table. Such proceeding enabled later reproduction of a scaffold structure and evaluating the improvement of scaffold adaptation to the biomechanical conditions.

The present procedure is a powerful searching tool which can be very useful to find implant structure best adapted to individual patient.

Bibliography

[1] ZGIERSKA A., *Wypadki przy pracy w 2007 r.,* Informacje i opracowania statystyczne – Departament Pracy i Warunków Życia, 2008.

[2] World Health Organization. *International statistical classification of diseases and related health problems 10th revision*, http://apps.who.int/classifications/apps/icd/icd10online/, 2007.

[3] VACCARO A.R., *The role of the osteoconductive scaffold in synthetic bone graft*, Orthopedics, May 2002, Vol. 25, No. 5, 571–578.

[4] BIAŁOZYK P., NIWINSKI P., FLADER A., *Wybrane problemy leczenia braków całkowitych uzębienia szczęki implantoprotezami stałymi*, Implantoprotetyka, 2008, Vol. IX, No. 3(32), 3–10.

[5] GOULET J.A., SENUNAS L.E., De SILVA G.L., GREENFIELD M.L., *Autogenous iliac crest bone graft. Complications and functional assessment*, Clin. Orthop. Relat. Res., 1997, Vol. 339, 76–81.

[6] BAUER T.W., MUSCHLER G.F., *Bone graft materials. An overview of the basic science*, Clin. Orthop. Relat. Res., 2000, Vol. 371, 10–27.

[7] JOSEPH J.R., WOODARD R., HILLDORE A.J., LAN S.K., PARK C.J., MORGAN J.A.C., EURELL A.W., CLARK S.G., WHEELER M.B., JAMISON R.D., JOHNSON A.J.W., *The mechanical properties and osteoconductivity of hydroxyapatite bone scaffolds with multi-scale porosity*, Biomaterials, 2007, Vol. 28, 45–54.

[8] LEE C.H., SINGLA A., LEE Y., *Biomedical applications of collagen*, Int. J. Pharm., 2001, Vol. 221, 1–22.

[9] DOMINIAK M., GERBER-LESZCZYSZYN H., *Rekonstrukcja podłoża protetycznego za pomocą plastyki wyrostka zębodołowego szczęki i żuchwy*, Adv. Clin. Exp. Med., 2005, Vol. 14, No. 3, 593–601.

[10] PŁOMINSKI J., KWIATKOWSKI K., *Przeszczepy kostne*, Pol. Merk. Lek., 2006, Vol. XXI, No. 126, 507–510.

[11] CANCEDDA R., BIANCHI G., DERUBEIS A., QUARTO R., *Cell therapy for bone disease: a reviev of current status*, Stem Cells, 2003, Vol. 21, 610–619.

[12] KAIGLER D., KREBSBACH P.H., WANG Z., WEST E.R., HORGER K., MOONEY D.J., *Transplanted endothelial cells enhance orthotopic bone regeneration*, J. Dent. Res., 2006, Vol. 85, No. 7, 633–637.

[13] CRISTOFOLINI L., VICECONTI M., *Mechanical validation of whole bone composite tibia models*, Journal of Biomechanics, 2000, Vol. 33, 279–288.

[14] HURWITZ D.E., SUMNER D.R., ANDRIACCHI T.P., SUGAR D.A., *Dynamic knee loads during gait predict proximal tibial bone distribution*, Journal of Biomechanics, 1998, Vol. 27, 423–430.

[15] MAQUET P.G.J., *Biomechanics of the Knee*, Springer-Verlag, second edition, 1984.

[16] ŚCIGAŁA K., *Badania modelowe charakterystyk odkształceniowych stawu kolanowego*, praca doktorska, Zakład Inżynierii Biomedycznej i Mechaniki Eksperymentalnej, Politechnika Wrocławska, 2002.

[17] CARTER D.R., BEAUPRÉ G.S., *Skeletal function and form*, Cambridge University Press, 2001.

[18] MARTIN R.B., *Porosity and specific surface of bone*, Crit. Rev. Biomed. Eng., 1984, 10(3), 179–222.

[19] SIVANANDAM S.N., DEEPA S.N., *Introduction to genetic algorithms*, Springer, 2008.

[20] HUTMACHER D.W., *Scaffolds in tissue engineering bone and cartilage*, Biomaterials, 2000, Vol. 21, 2529–2543.

[21] HOLLISTER S.J., MADDOX R.D., TABOAS J.M., *Optimal design and fabrication of scaffolds to mimic tissue properties and satisfy biological constraints*, Biomaterials, 2002, Vol. 23, 4095–4103.